Fluid-flow pressure measurements and thermo-fluid characterization of a single loop two-phase passive heat transfer device

IOP Conf. Series: Journal of Physics: Conf. Series **923** (2017) 012022 doi:10.1088/1742-6596/923/1/012022

Fluid-flow pressure measurements and thermo-fluid characterization of a single loop two-phase passive heat transfer device

A Ilinca[1], D Mangini[2], M Mameli[3], D Fioriti[3], S Filippeschi[3], L Araneo[4], N Roth[1], M Marengo[2]

[1] University of Stuttgart, Pfaffenwaldring 31, 70569 Stuttgart, Germany

[2]University of Brighton, Cockcroft Building, Lewes Road, Brighton BN2 4GJ, UK

[3] University of Pisa, Largo Lucio Lazzarino 2, 56122 Pisa, Italy

[4]Politecnico di Milano, Energy Department - Via Lambruschini, 4A - 20156 - Milan, Italy

E-mail: D.Mangini@brighton.ac.uk

Abstract. A Novel Single Loop Pulsating Heat Pipe (SLPHP), with an inner diameter of 2 mm, filled up with two working fluids (Ethanol and FC-72, Filling Ratio of 60%), is tested in Bottom Heated mode varying the heating power and the orientation. The static confinement diameter for Ethanol and FC-72, respectively 3.4 mm and 1.7mm, is above and slightly under the inner diameter of the tube. This is important for a better understanding of the working principle of the device very close to the limit between the Loop Thermosyphon and Pulsating Heat Pipe working modes. With respect to previous SLPHP experiments found in the literature, such device is designed with two transparent inserts mounted between the evaporator and the condenser allowing direct fluid flow visualization. Two highly accurate pressure transducers permit local pressure measurements just at the edges of one of the transparent inserts. Additionally, three heating elements are controlled independently, so as to vary the heating distribution at the evaporator. It is found that peculiar heating distributions promote the slug/plug flow motion in a preferential direction, increasing the device overall performance. Pressure measurements point out that the pressure drop between the evaporator and the condenser are related to the flow pattern. Furthermore, at high heat inputs, the flow regimes recorded for the two fluids are very similar, stressing that, when the dynamic effects start to play a major role in the system, the device classification between Loop Thermosyphon and Pulsating Heat Pipe is not that sharp anymore.

Keywords: Pulsating Heat Pipe, Loop Thermosyphon, Fluid flow Analysis, Local pressure measurements.

1. INTRODUCTION

As modern computer chips and power electronics become more powerful and compact, the need of more efficient cooling systems increases day by day. In the present scenario, Pulsating Heat Pipes (PHPs) are relatively new wickless two-phase passive heat transfer device that aim at meeting all the present and future thermal requirements [1][2]. Although the peculiar advantages of this emergent technology, such as its compactness, the possibility to dissipate high heat fluxes and the ability to

work also in microgravity conditions, the PHPs governing phenomena are quite unique and not completely understood [3].

Since the Single Loop PHP (SLPHP) can be considered the basic constituent of a multi-turn Pulsating Heat Pipes, its full thermo-fluidic characterization is fundamental for the complete description of the PHP or Thermosyphon working principles. At present, several studies contribute to the SLPHP knowledge [4][5][6][7] but further work is needed to understand the pressure evolution within PHPs coupled with the fluid flow visualization. For these main reasons, a novel SLPHP could provide vital information when performing simultaneous measurements with different refrigerant fluids on visualization of the fluid flow with a high-resolution camera, detection of the fluid temperature distribution during operation and the fluid pressure evolution both in the heated and in the cooled section. Considering that the inner diameter of the tube of 2 mm is slightly larger than the static confinement diameter for the FC-72 of 1.7 mm, the SLPHP can work theoretically as a thermosiphon. In static conditions, the FC-72 resides at the bottom of the device due to the gravity assistance and the lack of the capillary effects.

The aim of the work is to provide useful information on the basic phenomena involved, improving the PHP understanding. It is intended to demonstrate that a two-phase heat transfer device filled with two different fluids, FC-72 and Ethanol, each of them with static confinement diameter slightly under and slightly above the critical inner diameter in static conditions, have similar working mode during operation. This arise an open point in the literature on the need of more accurate criteria for the definition of the limits between Loop Thermosyphons [8] and Pulsating Heat Pipes. Finally, such experimental analysis provides accurate information for the validation of PHP numerical codes.

2. EXPERIMENTAL APPARATUS AND PROCEDURE

The basic features of the SLPHP are shown in Fig. 1a. The evaporator and the condenser are made of copper tubes (Inner diameter 2 mm, Outer diameter 4 mm) in order to minimize the thermal resistance between the working fluid and respectively the heat source and heat sink. The loop is completed by two transparent vertical tubes (110 mm axial length, 2mm ID,), allowing high-speed visualization of the two-phase flow, The loop components are connected by means of brass joints and sealed by vacuum epoxy (Henkel Loctite® 9492).

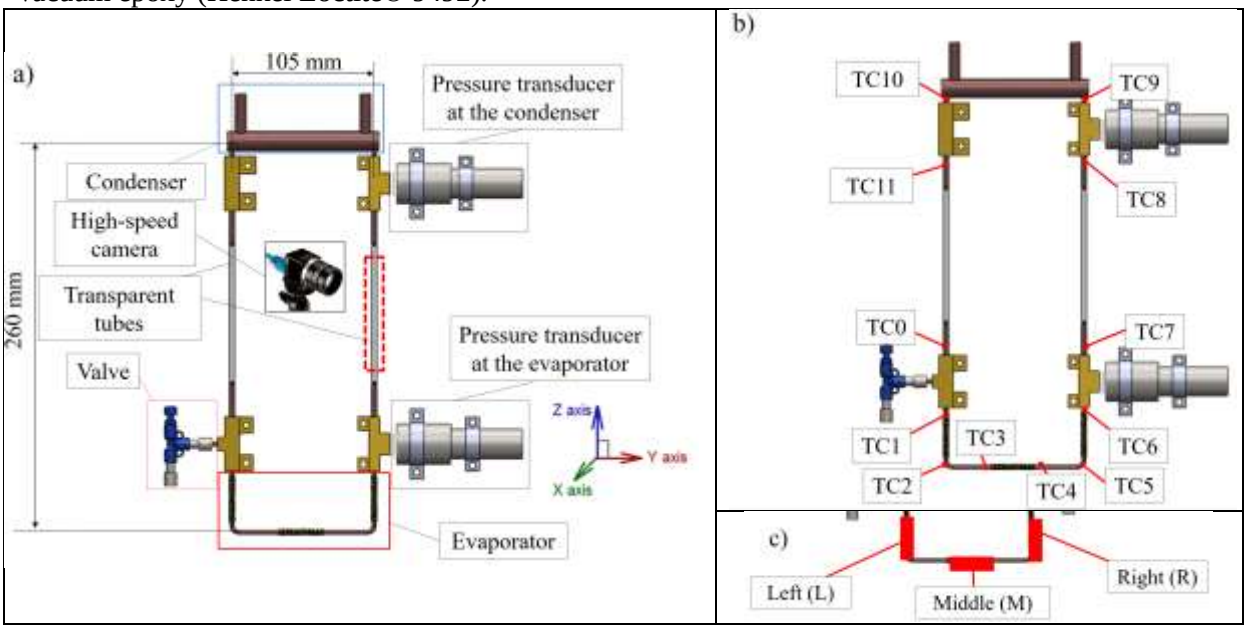

Figure 1. a) Main components of the SLPHP; b) Thermocouple positions; c) Heating elements positions

Two high-accurate pressure transducers (Keller® PX33, 1 bar Absolute, Accuracy 0.05% FSO), mounted just before and after one of the transparent inserts, measure the pressure drop along the adiabatic section.
The condenser section is embedded inside a mini shell and tube heat exchanger, directly connect to a thermal bath (Lauda® A300), recirculating water at 20 °C ±1 °C.

Three heating wires (Thermocoax®, Single core 1Nc Ac), are mounted in the evaporator section, providing a wall to fluid heat flux of 6.5 W/cm^2 at 10 W. The three heaters are controlled independently with a Pulse Width Modulation (PWM) control system, so as to vary the heating distribution along the heated zone. As shown in Fig. 1c, two heating elements (Heater L and Heater R) are positioned just above the 90° curves at the evaporator, in such a way, that by applying different power on them, the device is heated-up non-symmetrically with respect to the gravity field, while the Heater M is mounted at the center of the evaporator. As already demonstrated [9] for a similar multi-turn two-phase passive heat transfer device, when heating up the device non-uniformly at the evaporator with peculiar heating configurations, a circulation in a preferential direction is established, with a subsequent improvement of the overall thermal performance. Twelve T-type thermocouples measure the external wall temperature both in the heated and in the cooled region of the single loop (see Fig. 1c), while other two thermocouples monitor the environmental temperature during tests.

A data acquisition system (NI-cRIO-9074®, NI-9264®, NI-9214®, 2xNI-9205®, NI-9217®, NI-9472®) records the output of the thermocouples (at 10 Hz) and the pressure transducers (at 100 Hz). The high-speed camera (Ximea® USB3 XIQ-093, resolution 1280x1024 pixel) is connected to an ultra-compact PC (NUC® Board D54250WYB) able to store images up to 100 fps and it is synchronized via software with the pressure signals.

The device is vacuumed by means of an ultra-high vacuum system (Varian® DS42 and TV81-T) down to 0.3 mPa and then it is partially filled up with the working fluid with a volumetric ratio of 0.6 ± 0.03 (corresponding to 1.45 ml). Finally, the micro-metering (Upchurch Scientific® UP-P-447) valve that connects the SLPHP to the device is closed, guarantying a leak down to 10^{-8} mbar l/s. The fluid itself is previously degassed within a secondary tank, by continuous boiling and vacuuming cycles [10], in such a way to extract incondensable gases before the filling operation. Ethanol and FC-72 are choose as working fluids for their thermodynamic properties and for the fact that their critical diameter is very close to the inner diameter of the tube. The device filled up with Ethanol will act as a PHP; while with FC-72 will act as a compact loop thermosiphon.

Finally, a rotating structure was used in order to hold the device and incline it at different pivot angles, in order to aid for a faster start-up and promote the stabilization of the circulation. The pivot angle is defined and measured, referring to the laboratory fixed reference XYZ of Fig. 1a, as the rotation of the device around X-axis, counter-clockwise as seen in the figure.

3. EXPERIMENTAL RESULTS AND PROCEDURE

The experimental campaign is carried out in order to point out:

- the effect of the heating distribution on the overall thermal performance;
- the operational regimes in terms of fluid motion;
- the relationship between the pressure drop measurements and the flow patterns observed through the transparent insert;
- the uncertain limit between Loop Thermosyphon and Pulsating Heat Pipe in dynamic conditions for fluids whose static confinement diameter value is lightly lower and higher respectively than the inner diameter value of the tube.
- the effect of the pivot angle on the stabilization of the fluid circulation.

Tests are performed while maintaining the environmental temperature at 20°C ±1°C, inclining the device at four different pivot angles (vertical, 30°, 60° and 90°). The heating power is increased providing a global heating power levels of 1 W, 3 W, 6 W, 12 W and 18 W. For all the above levels, except 1 W, different heating configurations are tested: the heating power is split among the three heaters, to vary the heating distribution during tests. Pseudo-steady state conditions can be reached in

approximately 3 minutes, due to the low thermal inertia of the system. Nevertheless, all the heating configuration tested are kept constant for 15 minutes, to ensure that the device reaches the pseudo-steady state conditions for all the cases tested. A video sequence (20 seconds at 100 fps) is recorded during each tested combination of heat input power, pivot angle and working fluid. The video acquisition starts 13 minutes after each heat input power variation in order to wait for the pseudo-steady state conditions. The equivalent thermal resistance (R_{eq}) is evaluated as follows (Eq.1):

$$R_{eq} = \frac{\bar{T}_e - \bar{T}_c}{\dot{Q}_{tot}} \quad (1)$$

Where: $\dot{Q}_{tot}$ is the global heating power, which is the sum of the power of the three heaters: the Heater L ($\dot{Q}_L$), Heater M ($\dot{Q}_M$) and Heater R ($\dot{Q}_R$), as pointed out in the Eq. 2:

$$\dot{Q}_{tot} = \dot{Q}_L + \dot{Q}_M + \dot{Q}_R \quad (2)$$

Since each of the three heating elements, independently controlled, can provide a different heating power and for each of them two temperatures are measured as shown in fig. 1b, the averaged T_e is calculated as pointed out in the Eq. 3:

$$\bar{T}_e = \frac{\dot{Q}_L}{\dot{Q}_{tot}} \max(T_1; T_2) + \frac{\dot{Q}_M}{\dot{Q}_{tot}} \max(T_3; T_4) + \frac{\dot{Q}_R}{\dot{Q}_{tot}} \max(T_5; T_6) \quad (3)$$

$\bar{T}_c$ is the time average of TC9 and TC10 when pseudo-steady state conditions are reached.

A first test campaign is performed with Ethanol, with the device vertically oriented in Bottom Heated Mode, i.e. with the evaporator section below the condenser. For each heating configurations tested the overall temporal evolution of the temperatures and of the pressure recorded in the transparent section are shown in Fig. 2. Only 1 W is not sufficient to activate a self-sustained two-phase flow within the loop: the temperatures at the evaporator increases, while the pressure, close to the saturation pressure of ethanol at 20°C, exhibits a flat trend. When increasing the power at 3 W (Configuration 3a in Fig. 2a), the pressure signal points out some peaks, while the temperatures starts to decrease. In such period, the heating power activates a self-sustained two-phase flow motion, improving the heat transfer between the heated and the cooled sections of the device. However, at 3 W only partial start-ups are detectable: periods in which the two-phase flow oscillates between the heated and the cooled section are alternating with stop-over periods, where the fluid does not move, thus hindering the heat exchange. This is valid for all the configurations tested with a global heating input of 3 W (from 3a to 3e in Fig. 2a), independently from the heating configuration. When the total heating power of 6 W is provided to the heater M only (Configuration 6a) a full start-up is detected: after a sudden peak of pressure at the evaporator, the temperatures in the heated zone decrease abruptly to 35 °C.

a)

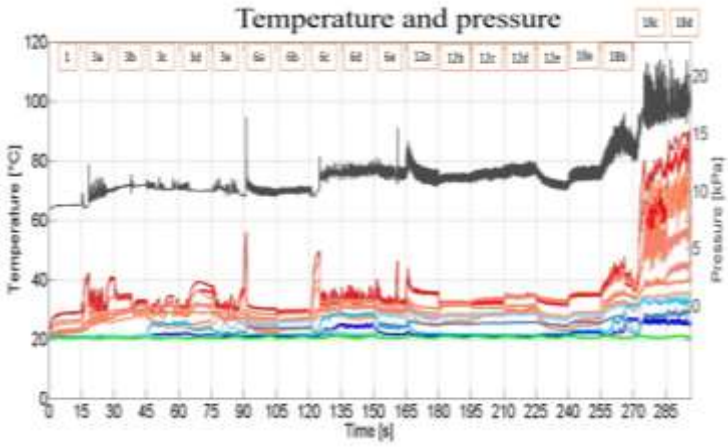

b)

Configuration	HEATER A [W]	HEATER B [W]	HEATER C [W]
1	0	1	0
3a	0	3	0
3b	1	1	1
3c	0	1	2
3d	0	1,5	1,5
3e	1,5	1,5	0
6a	0	6	0
6b	2	2	2
6c	1	2	3
6d	0	3	3
6e	3	3	0
12a	0	12	0
12b	4	4	4
12c	2	4	6
12d	0	6	6
12e	6	6	0
18a	9	9	0
18b	0	9	9
18c	4	6	8
18d	6	6	6

Figure 2. a) Temperatures and pressure evolution for Ethanol in vertical position;
b) Heating configurations sequence

This results in an improvement of the device thermal performance: the equivalent thermal resistance (R_{eq}) decreases down to 1 K/W, as observable in figure 4a. Interestingly, during the configuration 6a, a circulation of the two-phase flow that spontaneously follow a preferential direction was observed through the two transparent sections. The fluid visualization in Fig. 3 shows that an annular flow in the left transparent section flows continuously upwards from the evaporator to the condenser, while a slug/plug flow that preferentially falls from the condenser is detectable in the right transparent insert. Therefore, the TC10 and the TC11 show a higher value than the TC8 and the TC9, since the hot fluid from the evaporator is pushed preferentially through the left side of the loop. This circulation is obtained for the heating configurations 6a and 6b. Such two-phase flow motion in a preferential direction, ,improves the overall performance by continuously refreshing the hot section with a fluid flow that comes from the condenser with a lower temperature.

a) Clockwise motion

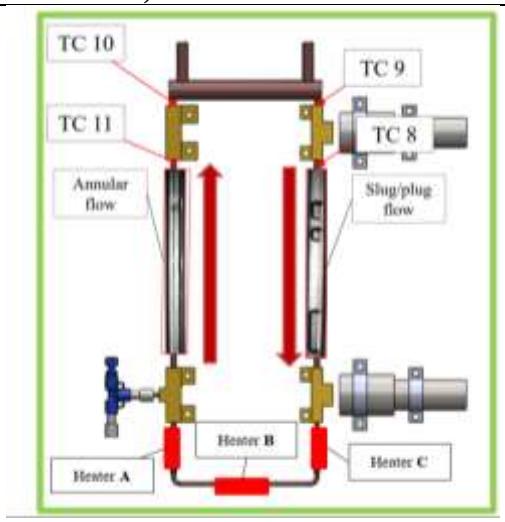

c) Temperature and pressure

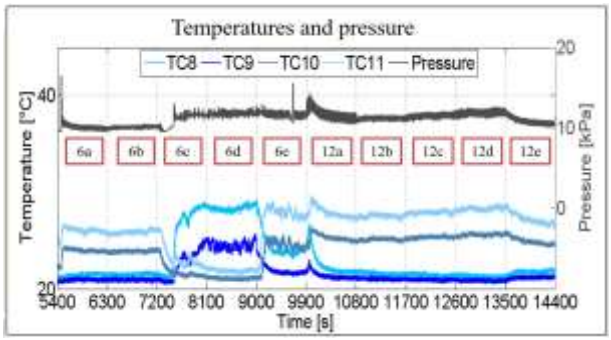

b) Anti-Clockwise motion

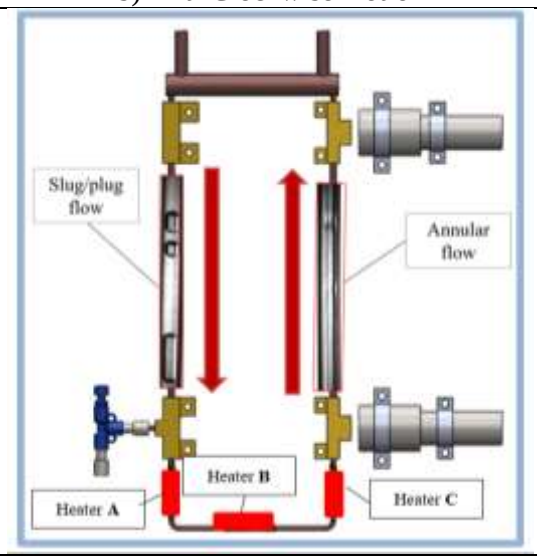

d) Test sequence with direction color coding

Config		Power Input (W)			Flow direction
		L	M	R	
6a	. ■ .	0	6	0	
6b	■■■	2	2	2	
6c	▂▄■	1	2	3	
6d	. ■■	0	3	3	
6e	■■ .	3	3	0	
12a	. ■ .	0	12	0	
12b	■■■	4	4	4	
12c	▂▄■	2	4	6	
12d	. ■■	0	6	6	
12e	■■ .	6	6	0	

Figure 3. Flow direction: a) clockwise circulation, green color in table d); b) Anti-clockwise, blue color in table d); c) temperatures and pressure in the condenser at 6 W and 12 W.

Therefore, the R_{eq} is every time close to 1 K/W. It is worthwhile to note that such circulation is achieved even when the system is heated up with a symmetrical configuration. This could be explained because the SLPHP is very sensitive to small hydraulic non-symmetries and to the higher thermal inertia of the components in the right side, such as the two stainless steel pressure transducers with a mass of 240 g each one. After switching from configuration 6b to 6c, the flow circulation reverses quickly visible from the increase of the temperature from TC8 and TC9. Now the annular flow that pushes upwards the fluid from the evaporator to the condenser is visible through the transparent section on the right side, while a slug/plug that goes preferentially from the evaporator to the condenser in the left one, as "anti-clockwise motion" (highlighted in the blue rectangular shape in Fig.3). This sudden variation of the circulation direction is due to the peculiar distribution of heating power provided by the configuration 6c: the local heating power provided to the Heater R is higher than the power dissipated by the Heater L and M. Therefore, the fluid is pushed preferentially through the right channel, changing the overall circulation direction. Therefore, the TC8 and the TC9 temperatures are for such configuration higher than the TC10 and the TC11. The Anti-Clockwise circulation is also observable during tests performed with the Configuration 6d: since the Heater L is off, the fluid is not pushed through the left side of the loop to the condenser. Changing from the Configuration 6d to the Configuration 6e, the fluid returns to move almost instantaneously following a Clock-wise orientation. During Configuration 6d, the Heater R is off, and therefore the fluid is not able to be pushed through the right side of the loop to the condenser. Interestingly, for such global heating power level of 6 W, the fluid motion is extremely sensitive to the peculiar heating distribution provided: a variation of the circulation direction is easily reachable providing a proper local heating power distribution in the heated region.

Increasing the global heating power from 6 W to 12 W (from the Configuration 12a to the Configuration 12e), the two-phase flow follows every time a "Clock-wise" direction, independently from the peculiar heating configuration at the evaporator. The TC10 and the TC11 are in fact every time higher than the TC9 and TC8 (Fig.4) and the annular flow that pushes continuously the fluid from the heated to the cooled region is always visible in the left transparent section. This could happen because, when increasing the global heat power input to dissipate, the fluid is pushed more vigorously from the heated to the cooled section of the device. The more heating power is provided, the higher the void fraction in the up header and the higher quantity of fluid in the down-comer. It is more difficult for the vapor expansion to contrast liquid column head and momentum. Therefore, once the circulation is established in the loop in a preferential direction for such heating power input, such inertial effect "dampens" the effect of the peculiar heating distribution provided at the evaporator, maintaining its direction for all the configurations tested.

Increasing further the global heating power from 12 W to 18 W, the temperatures at the evaporator increase abruptly, synonym of a thermal crisis (dry-out). The tests will be stopped as soon as the temperatures at the evaporator will reach 90°C in order to preserve the hardware integrity. At 18 W, in vertical position, the system is not able to switch the fluid flow direction between the different configurations tested. As soon as the configuration 18a is provided, the flow starts to oscillate without a preferential direction. The configuration 18a, being in contrast with respect to the "Clock-wise circulation" achieved for all the previous Configurations tested with a global heating power of 12 W, starts initially to push the fluid from the right section. Nevertheless, it is not able to change completely the fluid circulation: the two-phase flow starts to oscillate, and both the two transparent inserts are characterized by an oscillating semi-annular flow. At high heating powers, any attempt to force a flow reversal by changing the heating distribution, when a net flow circulation is already established, fails due to the combination of inertial effect and phase distribution. Therefore, only flow instabilities are detectable, that establish an oscillating flow, thus decreasing abruptly the overall performance. Therefore, the R_{eq} increases when a global heating power of 18 W is provided to the device (Fig.4a).

a) Ethanol, Vertical	b) Additional test up to 18 W

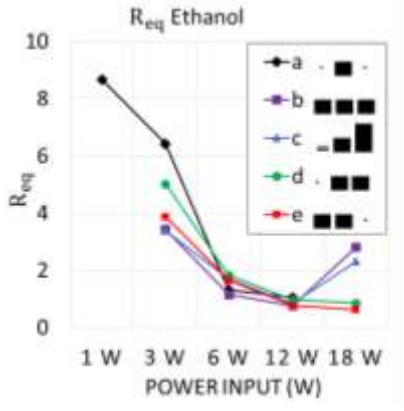

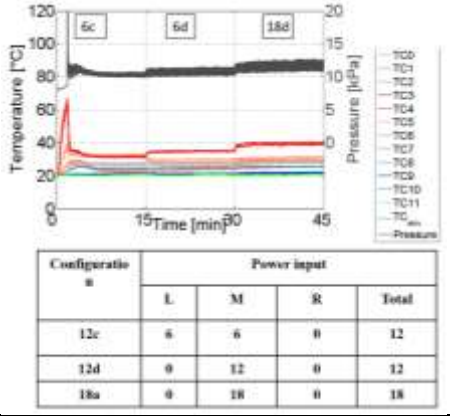

Configuration	Power input			
	L	M	R	Total
12c	6	6	0	12
12d	0	12	0	12
18a	0	18	0	18

Figure 4. a) Equivalent Thermal Resistance for all the heating distribution tested for long test with Ehanol in vertical position and b) Test performed providing to the device up to 18 W solely at the heater M.

a)

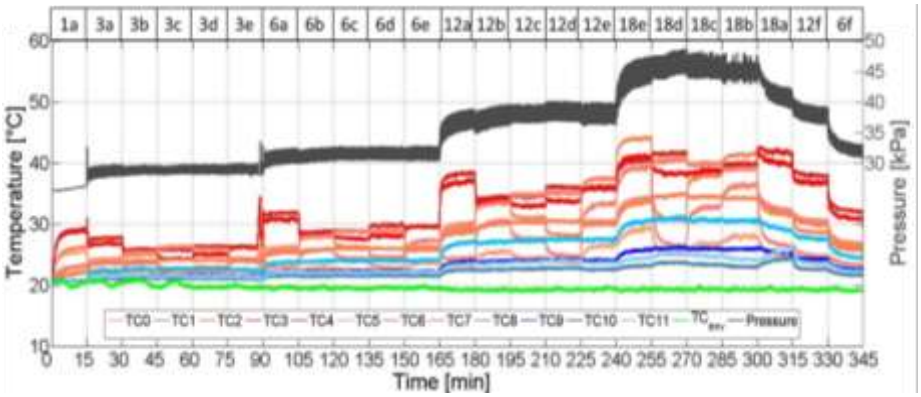

b)

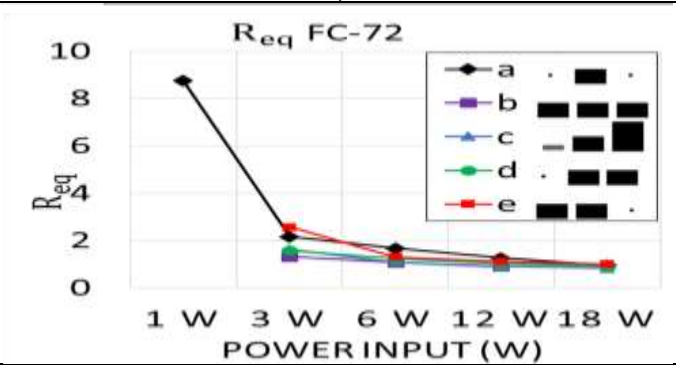

Figure 5. a) Temperatures and pressure evolution and b) Equivalent Thermal Resistance for all the heating distribution, test sequence with FC-72, 30° pivot angle

In order to check whether such thermal crisis is related to the relatively high power level, an additional test is performed, in which 18 W are dissipated solely from the Heater M (Fig. 4b), after the initiation of a self-sustained fluid flow circulation.

The maximum temperatures reached with 18 W are approximately 40°C. The heat exchange is also stable: the temporal evolution of the temperatures during such test reside in a narrow range of temperatures after the start-up, and a fluid circulation in a preferential direction is detectable through the transparent inserts. These results point out that the thermal crisis is not strictly related to the relatively high-power level but on the thermal history.

Similar results were obtained testing the device filled with FC-72 in vertical position, where already at 12 W, the system is not able to change the fluid flow direction between the 12d and 12e tested configurations resulting in a sudden increase of temperature and stop of the experiment.

Furthermore, testing the device filled with FC-72 fluid at a pivot angle of 30° for all the configurations from Fig. 2b, reveals that the pivot angle indeed helps to stabilize the fluid circulation, thus improving the overall performance (Fig. 5). From 6 W up to 18 W, the R_{eq} is every time close to 1 K/W.

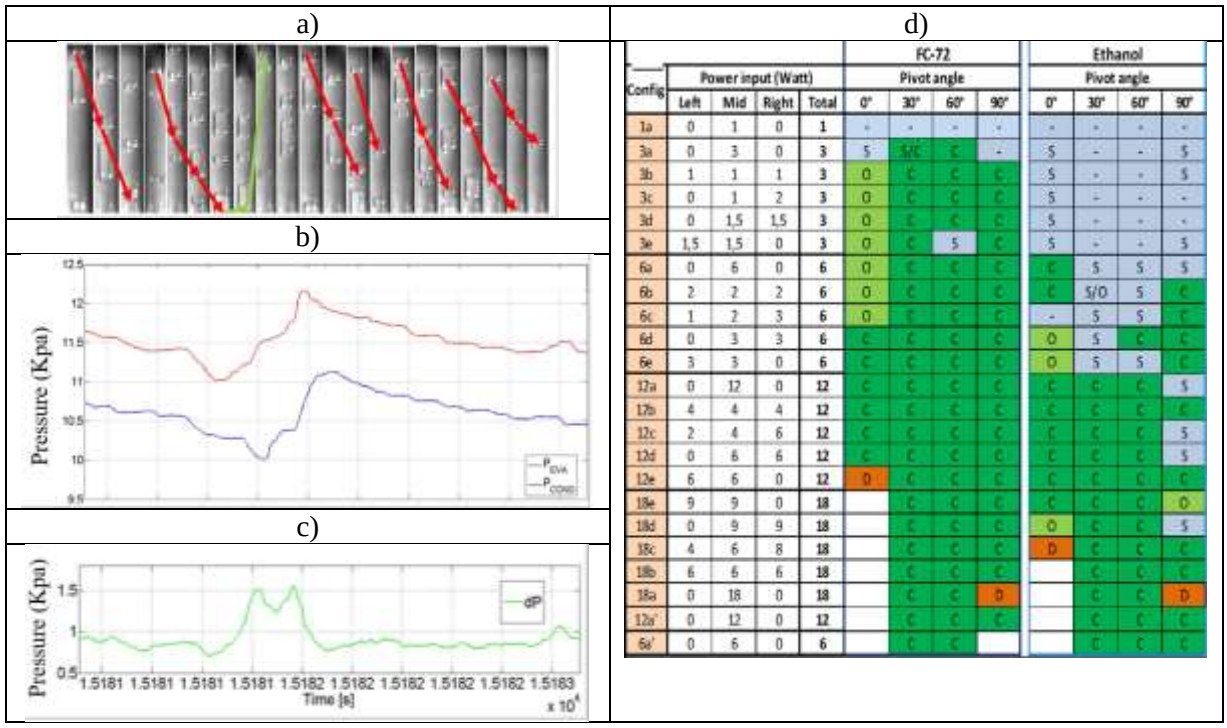

Config.	Power input (Watt)				FC-72 Pivot angle				Ethanol Pivot angle			
	Left	Mid	Right	Total	0°	30°	60°	90°	0°	30°	60°	90°
1a	0	1	0	1	-	-	-	-	-	-	-	-
3a	0	3	0	3	S	S/C	C	-	S	-	-	S
3b	1	1	1	3	O	C	C	C	S	-	-	S
3c	0	1	2	3	O	C	C	C	S	-	-	-
3d	0	1,5	1,5	3	O	C	C	C	S	-	-	-
3e	1,5	1,5	0	3	O	C	S	C	S	-	-	S
6a	0	6	0	6	O	C	C	C	C	S	S	S
6b	2	2	2	6	O	C	C	C	C	S/O	S	C
6c	1	2	3	6	O	C	C	C	-	S	S	C
6d	0	3	3	6	C	C	C	C	O	S	C	C
6e	3	3	0	6	C	C	C	C	O	S	S	C
12a	0	12	0	12	C	C	C	C	C	C	C	S
12b	4	4	4	12	C	C	C	C	C	C	C	C
12c	2	4	6	12	C	C	C	C	C	C	C	S
12d	0	6	6	12	C	C	C	C	C	C	C	S
12e	6	6	0	12	O	C	C	C	C	C	C	C
18e	9	9	0	18		C	C	C	C	C	C	O
18d	0	9	9	18		C	C	C	O	C	C	S
18c	4	6	8	18		C	C	C	O	C	C	C
18b	6	6	6	18		C	C	C		C	C	C
18a	0	18	0	18		C	C	O		C	C	O
12a'	0	12	0	12		C	C	C		C	C	C
6a'	0	6	0	6		C	C			C	C	C

Figure 6. Visualization and pressure drop synchronization of: a) the images taken with high speed camera, b) pressure measurements at the evaporator (red line) and at the condenser (blue line) and c) the pressure drop calculated; d) flow pattern map.

Fig. 6d resumes all the flow motions observed for all the pivot angles and fluids tested in a visually intuitive but also complete manner.

FC-72 working fluid has shown better thermal performances over the Ethanol since is it has a prompter start up reaching wider heat transfer capability range. The low boiling point of this liquid ensures the heat discharge to the condenser at low temperatures. An increase in pivot angle improves the flow conditions and broadens the operative range of the device for both fluids. This is due to the significant gravitational assistance and the particular geometry: the evaporator section is no longer horizontal, thus circulation is promoted also by applying power at the middle heater. Once the circulation is activated the performance of the system is very similar for both fluids reaching

temperatures in the range from 35 to 45 degrees for 12W and 18 W. The inertia of the fluid in this mode is so strong that the system is not sensitive at sudden changes neither to the distribution of the heat input. The fluid is rotating preferentially counter-clockwise because the configurations had been selected to promote the circulation in a preferential direction.

In Fig 6.d the legend is explained as:
" " no symbol = untested heating power level;
"-" = no fluid motion in the transparent tube;
"S" = start-up, shut down (unstable): flow may be stratified or weakly oscillating, with partial activation or deactivation of at least one heated section visible from the temperature readings;
"O" = oscillating (stable): a strong movement of fluid oscillating back and forth;
"C" = circulating (stable): a strong movement of fluid in one specific preferential direction;
"D" = dry-out: when excessive heat power input causes a thermal crisis in at least one evaporator section.

A synchronization between the images recorded in the transparent section and the pressure signals is performed and highlighted in Fig. 6.b. If a slug/plug flow is oscillating in the transparent section, the relationship between the fluid flow motion and the pressure measurements is clearly observable: when the two-phase flow is coming from the condenser section, the pressure decreases suddenly (sometimes of more than 500 Pa in less than 0.3 seconds) both at the evaporator and at the condenser. Nevertheless, when the flow is pushed from the heated to the cooled region during such flow reversal, a sudden increase of pressure is measured both at the evaporator and at the condenser.
It is observed that the peaks of pressure are more pronounced closer to the evaporator due to the expansions of the vapor bubbles, while at the condenser are smoother (Fig 6.b).

The pressure drop is also calculated, simply subtracting the pressure at the evaporator to the pressure measured at the condenser (Fig. 6c). The pressure difference is characterized by some peaks when fluid flow accelerations are detectable through the transparent section. Nevertheless, the static pressure difference depends on three main terms [11], as shown in Eq. 4:

$$\Delta P = \Delta P_f + \Delta P_a + \Delta P_g \tag{4}$$

where $\Delta P_f, \Delta P_a, \Delta P_g$ are relatively the friction, acceleration and static head terms. The hydrostatic pressure is dependent by the void fraction along the tube in which the pressure measurements are performed, that continuously change in time during PHP operations and it is also dependent by the peculiar flow pattern observed. Further analysis is needed to calculate the magnitude of the three components in Eq. 4.

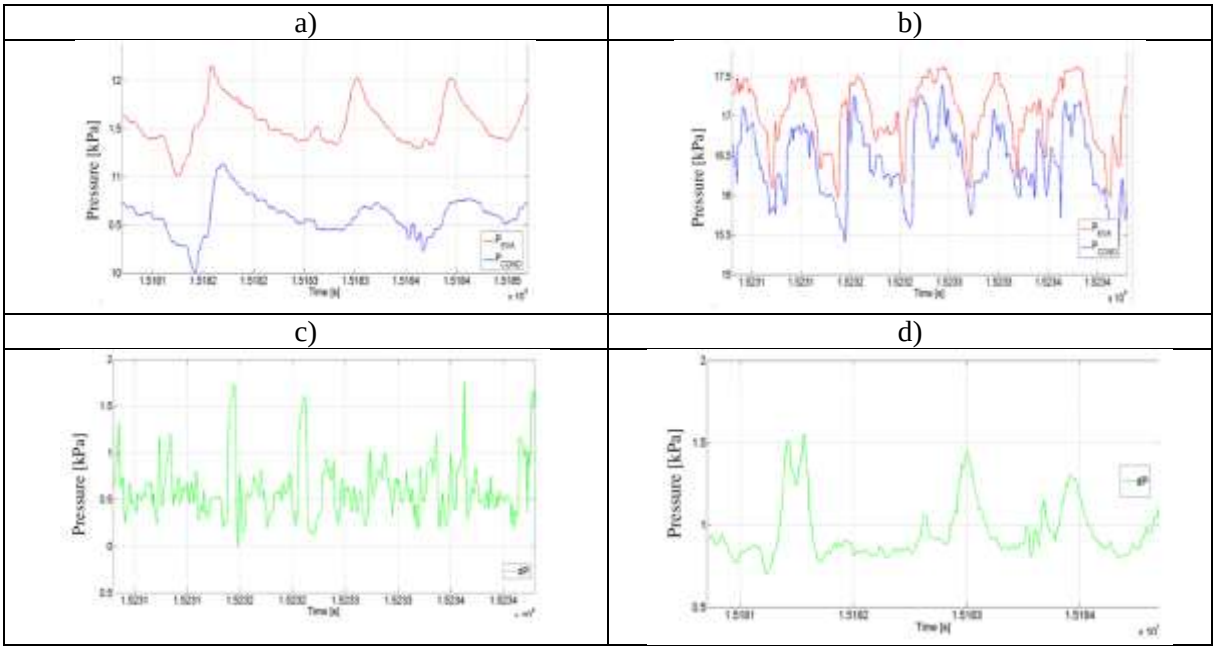

Figure 7. Pressure recorded just after the heated section (red line) and just before the cooled region (blue line) a) slug/plug flow; b) annular flow and Pressure drop measurements (green line) c) slug/plug flow; d) annular flow.

For instance, having the possibility to test the device in microgravity by means of parabolic flights, the hydrostatic pressure is not more present. The acceleration term may be estimated from the liquid velocity calculated by post-processing of the images recorded in the transparent section. In this way, it may be theoretically possible to calculate the pressure related to the skin friction, and to correlate it with respect to the peculiar flow pattern observed.
In the case of an annular flow, it is hard to find a relationship between the pressure measurements and the images recorded by the high-speed camera. In fact, it is difficult to track the annular flow evolution solely with the high-speed camera, since there are no liquid menisci to track as in the slug/plug flow case. The static head is nearly zero because the very small quantity of fluid in the tube, while the vapor acceleration term plays a major role. However, some aspects regarding the fluid-dynamic of the annular flow can be seen looking at the pressure signals during tests. The pressures measured when an annular flow pattern is shown in figure. 7b and 7d (pressure drop) are completely different with respect to the slug/plug flow case (Fig. 7a and Fig. 7c respectively). The oscillations have a higher frequency in time for the annular flow.

4. CONCLUSIONS

A Novel Single Loop Pulsating Heat Pipe, filled up with pure ethanol or FC-72 (Volumetric Filling Ratio = 60%) with an inner diameter value of 2 mm is tested with different heating power distribution and tilting angles. Three heating elements, mounted in strategic points of the evaporator, are controlled independently, in such a way to heat up the device varying the heating distribution. Furthermore, two highly accurate pressure transducers measure the pressure just at the edges of one of the transparent inserts.

Results point out that peculiar heating configurations stabilize the two-phase flow motion in a preferential direction, thus improving the overall performance and it was demonstrated that two fluids, FC-72 and Ethanol, with diameter respectively slightly below and above the critical value, behave respectively as a thermosiphon or as a PHP in static conditions, but show similar working modes

during dynamic operation. Moreover, an increase in inclination, improves the flow conditions and broadens the operative range of the device for both fluids.

The pressure measurements recorded just after the heated and before the cooled section highlights that the pressure evolution is strictly dependent on the flow pattern observed. Qualitatively, each flow pattern always exhibits a pressure difference that can be correlated to fluid velocity and acceleration, static head terms, void fraction, fluid density and friction. When a slug/plug flow is observed through the transparent section between the two pressure transducers, the difference of pressure reaches 1.5 kPa and the pressure oscillations exhibit a lower frequency. When annular flow is detected, the pressure variations between the heated and the cooled section are less than the slug/plug flow case, but with higher frequency.

Such high speed visualization coupled with the highly accurate pressure measurements performed in this work, regarding the liquid film evolution, could provide useful information for updating and validating the actual lumped parameters models [12][13] and the emerging Computational Fluid Dynamic simulations on PHPs [14][15].

5. NOMENCLATURE

FC-72 Perfluoro-hexane
Heater-L the heater on the Left side
Heater-M the heater in the Middle, central position
Heater-R the heater on the Right side
P_{EVA} Fluid Pressure measured close to the evaporator
P_{COND} Fluid Pressure measured close to the condenser
PHP Pulsating Heat Pipe
pivot angle the device rotation angle around its X-axis, counter-clockwise
Q'_{L} power of the Left heater
Q'_{M} power of the Median heater
Q'_{R} power of the Right heater
Q'_{TOT} total power of the three heaters
R_{eq} equivalent thermal resistance
SLPHP Single Loop Pulsating Heat Pipe
T_c average temperature at the Condenser
T_e average temperature at the Evaporator
TC_{env} environment thermocouple or temperature
TC_N thermocouple number N ($0 \leq N \leq 11$) or its recorded temperature
ΔP total pressure difference
ΔP_f friction pressure difference
ΔP_a acceleration pressure difference
ΔP_g static gravitational pressure difference

6. REFERENCES

[1] Akachi H. 1990 US Patent 4.921.041.
[2] Akachi H. 1993 US Patent 5.219.020.
[3] Zhang Y. and Faghri A. 2008 *Heat Transfer Eng.* **29** 20-44.
[4] Khandekar S. and Groll M. 2004 *Int. J. of Therm.Sci.* **43** 13-20.
[5] Khandekar S., Gautam A. P. and Sharma P. 2009 *Int. J. of Therm. Sci.* **48** 535–546.
[6] Spinato G., Borani N. and Thome J. R. 2015 *Energy* **90** 889–899.
[7] Spinato G., Borani N. and Thome J. R. 2016, *Int. J. of Therm. Sci.* **102** 78–88.
[8] Mangini D, Mameli M, Fioriti D, Filippeschi S, Araneo L and Marengo M 2017, *Appl.Therm. Eng.* **126** 1029-1043.
[9] Mameli M, Mangini D, Vanoli G, Filippeschi S, Araneo L and Marengo M 2016 . *Energy* **112** 562–573.

[10] Henry C.D, Kim J and Chamberlain B 2004, *3rd Int.Symp. on Two-Phase Flow model. and Exp.* Pisa, Italy
[11] Collier G and Thome J R 1994, Oxford Science Publications, third edition.
[12] Nekrashevych I and Nikolayev V. S 2017 *Appl. Therm. Eng.* **117** 24-29.
[13] Manzoni M, Mameli M, de Falco C, Araneo L and Marengo M 2016 , *Int. J. for Num.Meth. in Fl.* **82(7)** 375–397.
[14] Jiaqiang E, Zhao X, Deng Y and Zhu H, 2015. *Appl. Therm. Eng.* **93** 166–173.
[15] Pouryoussefi S M. and Zhang Y 2015 *Appl. Therm. Eng.* **98** 617-627.